






Article

Investigating Sedimentation Behavior of Montmorillonite Flocs between Flat Plates in a 2D System Using Image Analysis

Md Roknujjaman ¹, Keisuke Yoshida ², Muhamad Ezral Bin Ghazali ¹, Jiawei Li ¹, Harumichi Kyotoh ², Yasuhisa Adachi ¹ and Yohei Asada ^{1,*}

¹ Faculty of Life and Environmental Sciences, University of Tsukuba, Tsukuba 305-8572, Japan; rkripon.mathiu@gmail.com (M.R.); lijiaaweiwin@163.com (J.L.); adachi.yasuhisa.gu@u.tsukuba.ac.jp (Y.A.)
² Department of Engineering Mechanics and Energy, University of Tsukuba, Tsukuba 305-8573, Japan; harumichi.kyotoh@gmail.com (H.K.)
 * Correspondence: asada.yohei.ga@u.tsukuba.ac.jp; Tel.: +81-80-1489-2974

Abstract: The sedimentation of flocs in aquatic environments is a fundamental phenomenon that has not yet been fully elucidated. This study quantitatively examines sedimentation behavior, particularly focusing on sedimentation turbulence, in a two-dimensional system between flat plates, utilizing image analysis. Experiments were conducted in a rectangular container with montmorillonite suspensions coagulated in a sodium chloride solution. The settling motion of flocs was visualized using a green laser from above and captured horizontally with a digital camera. The study employed Particle Image Velocimetry (PIV) to analyze the velocity field in floc sedimentation, using the flocs as tracers to calculate the mean velocity at the sediment–supernatant interface. The results showed that the mean PIV value is affected by rising particles caused by sedimentation turbulence, indicating that PIV analysis of flow fields using flocs as tracers is reliable. The maximum settling velocity was found to increase with the initial interface height and the thickness of the container. The study further notes that flow velocity fluctuations increase during rapid sedimentation, marked by repeated collisions, separation, and the flocculation of variably sized flocs, offering a clear explanation of sedimentation turbulence. Additionally, Fourier analysis of vertical spectra in the container reflects the formation and collapse of flocs.

Keywords: montmorillonite flocs; sedimentation; formation and collapse; sedimentation turbulence; PIV; Fourier transformation



Citation: Roknujjaman, M.; Yoshida, K.; Bin Ghazali, M.E.; Li, J.; Kyotoh, H.; Adachi, Y.; Asada, Y. Investigating Sedimentation Behavior of Montmorillonite Flocs between Flat Plates in a 2D System Using Image Analysis. *Processes* **2024**, *12*, 295. <https://doi.org/10.3390/pr12020295>

Academic Editor: Li Xi

Received: 8 January 2024

Revised: 25 January 2024

Accepted: 27 January 2024

Published: 30 January 2024



Copyright: © 2024 by the authors. Licensee MDPI, Basel, Switzerland. This article is an open access article distributed under the terms and conditions of the Creative Commons Attribution (CC BY) license (<https://creativecommons.org/licenses/by/4.0/>).

1. Introduction

Colloidal substances are ubiquitous in aquatic environments. Their sedimentation behavior plays crucial roles in the solid–liquid separation process, such as water treatment, and the transportation of cohesive sediment in rivers and estuaries [1–4]. Although these substances, the majority of which exist as flocs in natural water environments—are important in sanitary, river, and coastal engineering, the sedimentation behavior of floc suspensions has been largely overlooked. This phenomenon is frequently observed in paddy field agriculture [5]. During the plowing and puddling periods of the irrigation process, chemicals from fertilizers adsorb onto the surfaces of clay particles within the flocculated sediments of paddy fields. These chemicals are subsequently discharged from the paddy fields into irrigation drainage channels through both the percolation and overflow of paddy water, thereby contributing to the contamination of river water [6,7]. Such contaminants can endanger entire ecosystems [8]. Therefore, flocs are considerably more important transport units than individual particles, influencing diverse environmental phenomena. Given these factors, the settling process of flocs under gravity is considered one of the most fundamental yet unexplored issues in understanding the transport of chemicals through water. The behavior of flocs is classified into three regimes based on their effective concentration [9]. In the dilute regime, the formed flocs settle relatively

freely; larger flocs settle more quickly, while smaller flocs settle more slowly, and there is no clear demarcation between the sediment and the supernatant. In the semi-dilute regime, a network-like structure emerges from the mutual interactions between flocs, leading to sluggish settling before rapid sedimentation begins. This interaction creates a distinct boundary between the sediment and the supernatant, as smaller flocs are often entrapped within the larger floc-formed networks. Following this, the flocs start to settle rapidly because of floc collapse, forming a sediment layer at the bottom that eventually consolidates under gravitational forces. In contrast, in the high-concentration regime, consolidation occurs predominantly within the initially formed flocculated sediment network structure. In the present study, our focus is on the sedimentation behavior of the semi-dilute regime.

Over the past decades, the sedimentation phenomena of various types of particles have been studied; Kynch first established a theoretical framework for sedimentation [10]. However, this theory was developed based on monodispersed, non-colloidal materials [11], and thus, it does not accurately describe the sedimentation of flocculated materials [12]. In 1954, Richardson and Zaki studied the hindered settling of monodispersed fluidized beds and established the well-known Richardson and Zaki equation to describe bed expansion, which is used in various industries [13]. Later, in 1962, Michaels and Bolger demonstrated that the sedimentation equation could be applied to the flocculated clay suspension (kaolin-ite in their case) in the dilute regime [14]. However, to apply this equation, we must assume a representative size and settling velocity for flocs. Additionally, they reported a tendency for the maximum settling velocity to be influenced by the initial height of the suspension, a finding also observed in our previous study on flocculated montmorillonite [15,16]. This phenomenon has been identified as the feed-forward mechanism of sedimentation turbulence [15,17]. This mechanism can be described as follows: large flocs settle rapidly, leading to collisions with smaller flocs due to differences in settling velocities. These collisions contribute to the growth of larger flocs, thereby fostering the downward movement of flocculated sediment and the upward motion of fluid. Sedimentation is accelerated by the growth of larger flocs, and conversely, the growth of larger flocs is facilitated by the process of sedimentation. The repetition of this sequence leads to rapid sedimentation and turbulent flow. Increasing the initial height of the suspension allows for a longer settling distance, which, in turn, increases the likelihood of collisions between settling flocs. This promotes the growth of larger flocs and enhances the sedimentation process. Therefore, the increase in maximum settling velocity with the initial height can be attributed to sedimentation turbulence. However, few studies have quantitatively evaluated such settling behavior, except for the measurement of settling velocity at the interface.

Montmorillonite is a type of alkaline clay [18,19]. An aqueous suspension of montmorillonite particles is readily flocculated upon the addition of NaCl. In addition, montmorillonite flocs can be enlarged by increasing the concentration of NaCl, making them very suitable for analyzing the sedimentation behavior of flocculated materials. Given its semi-transparent nature, the formed flocculated suspension of montmorillonite can be easily observed by illuminating a laser sheet. For these reasons, an aqueous suspension of montmorillonite particles coagulated in a high NaCl concentration can be regarded as one of the best models for observing and analyzing the sedimentation behavior of flocculated materials.

Particle Image Velocimetry (PIV) is a popular and well-developed technique in hydraulic engineering and fluid sciences used to measure the velocity field of fluid flow in elapsed time. It has been utilized in previous research to study various turbulent phenomena in laboratory experiments [20]. In this study, we employed PIV analysis to investigate the two-dimensional sedimentation behavior of montmorillonite flocs, including the characteristics of sedimentation turbulence phenomena, within a rectangular container. The study also explored the effects of the physical constraints of rectangular containers on sedimentation behavior, with different initial interface heights and varying container thicknesses. Additionally, Fourier analysis was introduced to estimate floc size. The remainder of this paper is organized as follows: Section 2 describes the experimental setup, materials,

and image analysis. Section 3 presents the experimental results and discussion. Section 4 provides the conclusions.

2. Experiments

The sedimentation behavior of montmorillonite flocs between flat plates in a 2D system was explored using Particle Image Velocimetry (PIV) analysis. For this purpose, the experimental apparatus consisted of a rectangular container. A laser sheet, specifically, a Nd:YAG laser (LA-D40-CW from Omicron, Erlangen, Germany) illuminated the flocculated sedimentation of the montmorillonite suspension within each container, thereby facilitating a 2D system analysis. The experiment utilized a mixture of water, montmorillonite gel, and sodium chloride solution. Section 2.1 details the experimental setup and materials, and Section 2.2 delves into the image analysis, encompassing PIV; PTV; observation of the interface height; and Fourier transformation, as applied to the settling behavior of montmorillonite flocs.

2.1. Experimental Setup and Materials

The experimental arrangement, depicted in Figure 1, utilized a rectangular settling container measuring 120 mm in width and 500 mm in height and featured varying thicknesses of 10 mm, 15 mm, and 20 mm. The container was filled with a prepared flocculated Na-montmorillonite suspension. To illuminate the flocculated sedimentation of the montmorillonite within each container, a laser sheet from a Nd:YAG laser (LA-D40-CW; Omicron, Erlangen, Germany) was used. The sedimentation flow within this 2D system was captured using a NIKON D7200 digital camera (Nikon, Tokyo, Japan), operating at a frame rate of 30 frames per second (fps). For the purposes of this study, the Particle Image Velocimetry (PIV) technique was employed to capture a 2D flow field within a vertical plane. This approach allowed for the quantification of the two velocity components within the plane using a series of time-resolved images taken by the camera. In this experiment, montmorillonite (Kunipia-F) [21], commercially obtained from Kunimine Industries Co., Ltd. (Tokyo, Japan), was used as a flocculated material. The preparation of the montmorillonite sample and flocculated Na-montmorillonite was described in a paper by Ghazali et al. [15]. For the experiment, the working liquid comprised a mixture of water, montmorillonite gel, and sodium chloride solution. Initially, 18.86 g of montmorillonite gel was added to 1 L of water to create a volume fraction of 2.0×10^{-4} . Following this, 1 L of 2 M sodium chloride solution was added to the montmorillonite suspension, resulting in a 1 M NaCl montmorillonite suspension. We stirred the NaCl montmorillonite suspension in a separate container several times and then transferred it into the rectangular container to begin the experiment.

2.2. Image Analysis for Montmorillonite Floc Settling Behavior

In this study, the Particle Image Velocimetry (PIV) technique is utilized to analyze the settling behavior of montmorillonite flocs. PIV facilitates the capture of both two-dimensional and three-dimensional images within a single frame and identifies particles from one frame to the next using a multi-frame recording method [22]. We employed a PIV system comprising a camera coupled with image-processing software to quantify the well-described concept of sedimentation turbulence observed during the sedimentation of Na-montmorillonite flocs in a 2D flow. An extensive analysis of the flow velocity field, including parameters like mean velocity and velocity fluctuation, was conducted. The tracking of the settling particles, including those in unstable flow conditions, was accomplished by illuminating the laser sheet. As a result, the images were analyzed to determine the entire flow velocity field. Additionally, PIV analysis enables the determination of various parameters, including cross-sectional average flow velocity, vorticity, divergence, and velocity vectors. This makes it highly suitable for investigating the flow conditions of numerous particles within the system. In this study, we utilized PIVlab, an open-source MATLAB tool known for its excellent performance and minimal error rates. In addition

to ease of implementation and use, PIVlab provided accurate and reliable results [23]. For the analysis conducted in this study, 300 data points were acquired along the interface at regular intervals. Using these data points, the interfacial average flow velocity, \bar{v} , was calculated utilizing Equation (1).

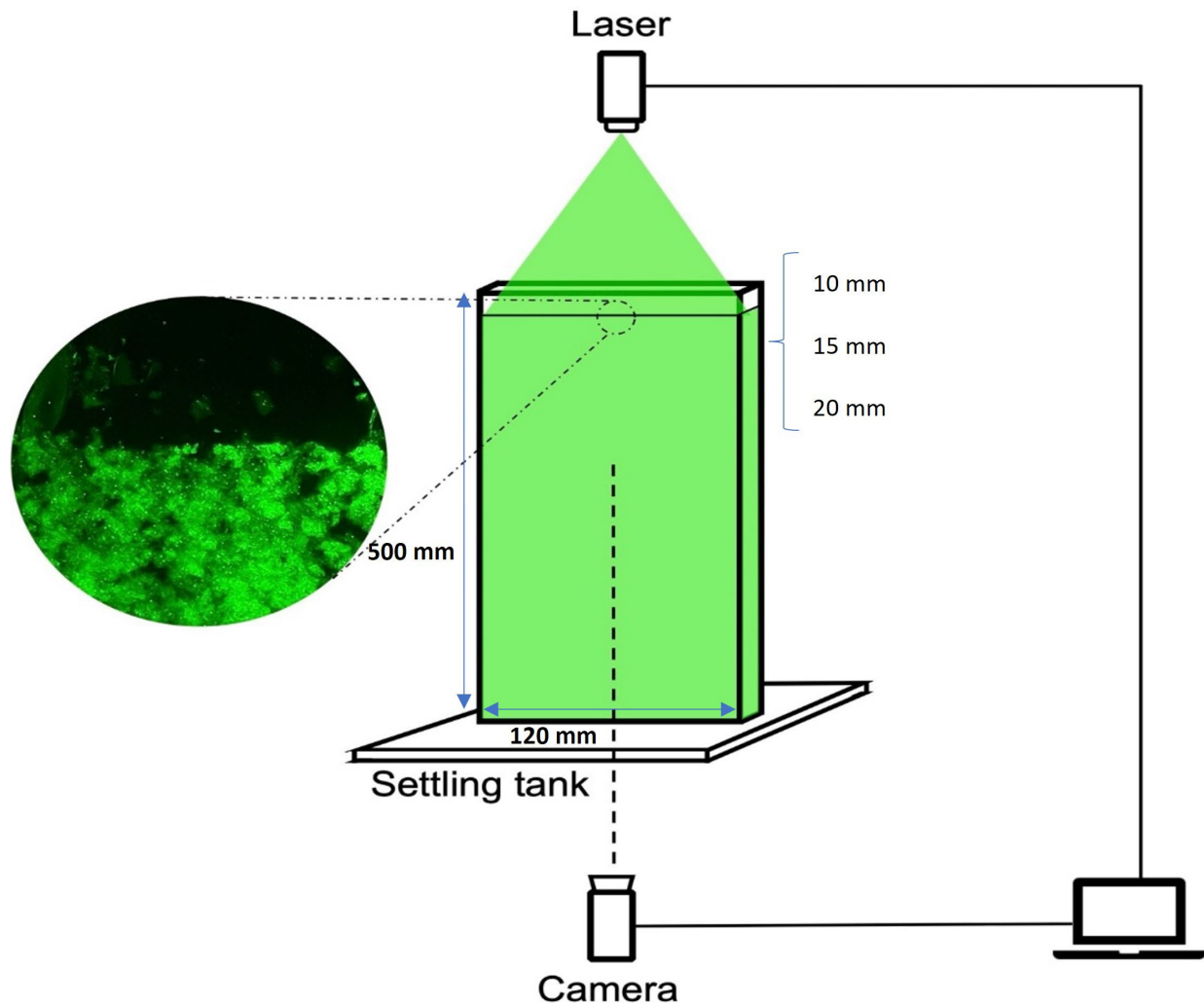


Figure 1. Schematic diagram of the experimental setup using PIV.

$$\bar{v} = \frac{1}{300} \sum_{i=1}^{300} v_i \quad (1)$$

where v_i is the flow velocity at each data point. The image data acquired from the experiment was also analyzed using Particle Tracking Velocimetry (PTV) to validate the results obtained from the PIV analysis. PTV analysis enables the selection and tracking of multiple particles of interest using the analysis software Move-tr/2D. For this purpose, three flocs situated near the interface were identified, and their settling velocities were measured. Consequently, the verification of the PIV analysis was carried out by comparing the interfacial average flow velocity obtained from the PIV analysis with the average settling velocity determined through PTV analysis. Additionally, the interface velocity was calculated based on the observation of the interface height. The interface height was determined by setting it at the lowest position of the interface line, with measurements conducted visually. The

interface velocity, v_h , was then calculated using a fourth-order accurate difference scheme based on the first derivative, as shown in Equation (2).

$$v_h = \frac{8h(t + \Delta t) - h(t - \Delta t) - h(t + 2\Delta t) - h(t - 2\Delta t)}{12\Delta t} \quad (2)$$

where $h(t)$ and Δt represent the interface height at time t and the time step, respectively. Furthermore, Fourier analysis was performed to investigate the growth of the flocs over time following image processing. The montmorillonite flocs experience growth through sedimentation and consolidation, which results in increased illumination. By taking this phenomenon into account, it was possible to quantify the growth of the flocs over time by analyzing the illumination intensity in the images using Fourier analysis. In this analysis, the Fourier transform was applied to calculate the spectrum and to quantitatively measure the floc size at the dominant wave number. The relationship between the wavelength (floc size in 2D), L (cm), and the wave number, f (cm^{-1}), is provided by Equation (3).

$$L = \frac{1}{f} \quad (3)$$

Furthermore, the angular wave number, $2\pi f$, is calculated by multiplying the wave number f by 2π . Utilizing this angular wave number, along with amplitude and time data, a three-dimensional graph can be generated to visually represent the changes and growth of the flocs over time.

3. Results and Discussion

The sedimentation behavior of montmorillonite flocs in the rectangular container was examined using PIV analysis. It was observed that the flow velocity obtained from the PIV analysis was smaller than those obtained from other methods. Additionally, sedimentation turbulence was observed during the settling of flocculated Na-montmorillonite flocs in a 2D flow. It was also noted that the maximum settling velocity increased with the initial interface height and thickness of the rectangular container. This section is organized as follows: Section 3.1 describes the sedimentation behavior of montmorillonite flocs over time, while Section 3.2 discusses the validity of the PIV analysis. Section 3.3 describes the sedimentation turbulence phenomenon in 2D using PIV analysis. In Section 3.4, the quantification of sedimentation turbulence using root-mean-square (RMS) velocity fluctuations is explained. In Section 3.5, the effects of initial interface height and container thickness on sedimentation behavior are discussed. Section 3.6 shows the floc size estimation conducted via Fourier analysis.

3.1. Sedimentation Behavior of Montmorillonite Flocs

Figure 2 represents the time variation in the interface height, while Figure 3 illustrates a time-lapse image describing the growth process of montmorillonite flocs during sedimentation in a container with a thickness of 20 mm. We observed that the initial 5 min of the experiment can be characterized as the flocculation stage. During this stage, the particles initially diffuse uniformly and gradually collide with surrounding particles, leading to the growth of flocs. At this stage, these interactions between flocs result in a slow decrease in the interface height. Following the flocculation stage, approximately from 5 min to 20 min, the settling stage occurs. In this stage, the floc interactions formed during the flocculation stage collapse, initiating rapid sedimentation. Larger flocs settle more quickly, leading to collisions between flocs with different settling velocities, promoting further floc growth and the development of a descending flow. Simultaneously, an upward flow of fluid is generated, enhancing the sedimentation process. This process, known as the feed-forward mechanism, is responsible for the rapid sedimentation. After the settling stage, a very slow consolidation commences as the flocs at the bottom start to compact under their own weight. This stage is referred to as the consolidation stage. Thus, settling phenomena for

montmorillonite flocs similar to those observed in a previous experiment in a cylindrical container [15] were successfully observed.

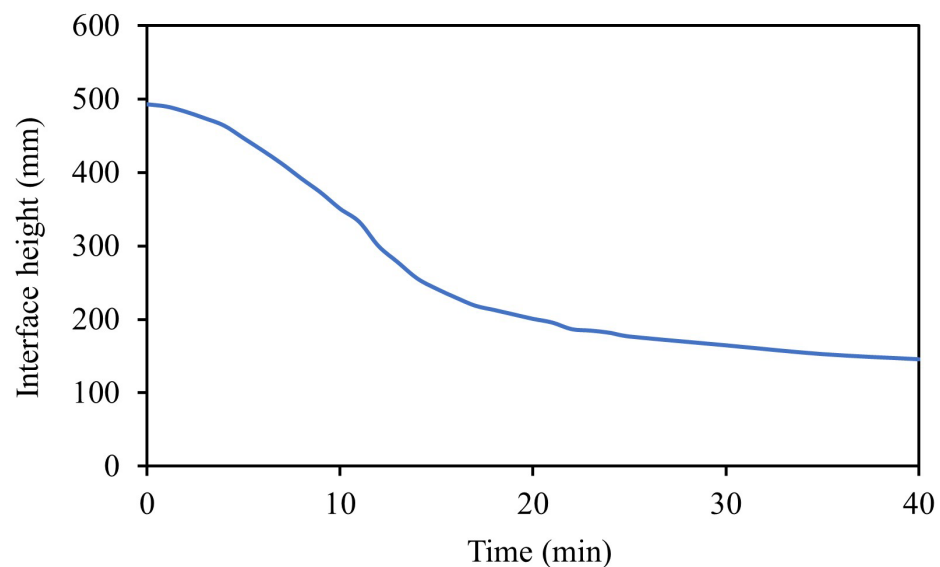


Figure 2. Time variation in the interface height during sedimentation in a container with a thickness of 20 mm.

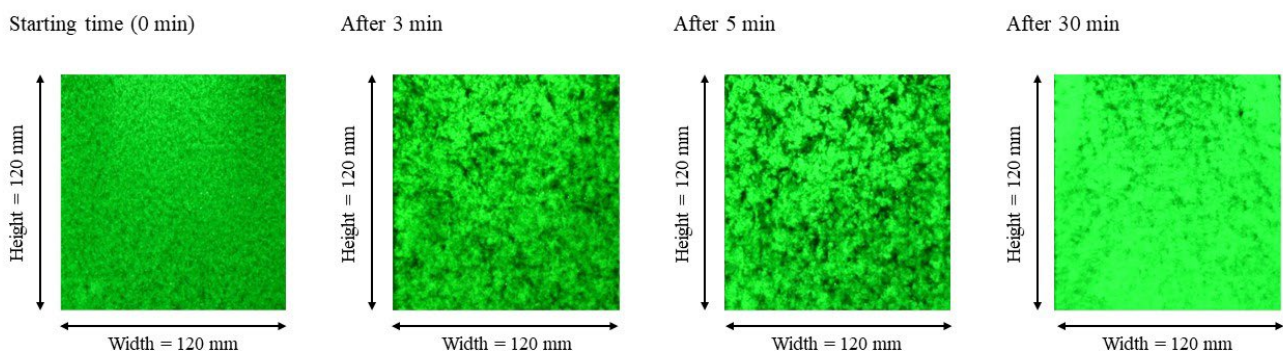


Figure 3. Time-lapse image describing the growth process of montmorillonite flocs during sedimentation in a container with a thickness of 20 mm.

3.2. Validation of PIV Analysis for Sedimentation Behavior

The time variations in the interfacial average velocity determined via PIV in the 20 mm rectangular container are presented in Figure 4. Figure 4a represents a comparison of interfacial average velocity calculated via PIV and PTV and interface velocity based on the observation of the interface height. As depicted in Figure 4a, it is evident that the flow velocity changes over time, and all the characteristic features of flocculation, sedimentation, and consolidation stages are consistent with previous studies [15]. However, when comparing the value of flow velocity obtained with different analysis methods, a discrepancy is noted. The flow velocity obtained from the PIV analysis is found to be smaller than those obtained from other methods. This discrepancy can be attributed to the lifting of smaller flocs vertically due to sedimentation turbulence. Since PIV analysis captures upward flow velocity points, it is anticipated that the obtained average values will be smaller. To address this issue, as shown in Figure 4b, the interfacial average flow velocity obtained using PIV analysis was recalculated by excluding the upward flow velocity points from the 300 velocity points. Upon recalibration, it was observed that the corrected values of interfacial average flow velocity increased compared with the original values across the overall time series. However, they remained smaller than the average flow velocities

obtained from the PTV analysis and the interface velocities based on the observation of the interface height. The maximum flow velocities of all the interfacial velocities obtained with the PIV analysis have also been incorporated into Figure 4b. It was noted that the maximum flow velocities were significantly high, indicating that the analysis was capable of tracking even high-velocity particles. However, the presence of numerous measurement points with low flow velocity was also observed. This could be because the flow velocity at each measurement point in PIV is derived by averaging the flow velocities around the measurement point, which could be influenced by flocs moving in the opposite direction of settling, as illustrated in Figure 5. Similarly, in PTV analysis, multiple flocs near the interface are selected and averaged, which could introduce errors. Despite the inherent errors associated with each analysis method, the consecutive characteristics of flow velocity variation were found to be consistent across all methods. This consistency suggests that the results obtained from the PIV analysis are reliable and validate its effectiveness in studying the sedimentation behavior of montmorillonite flocs.

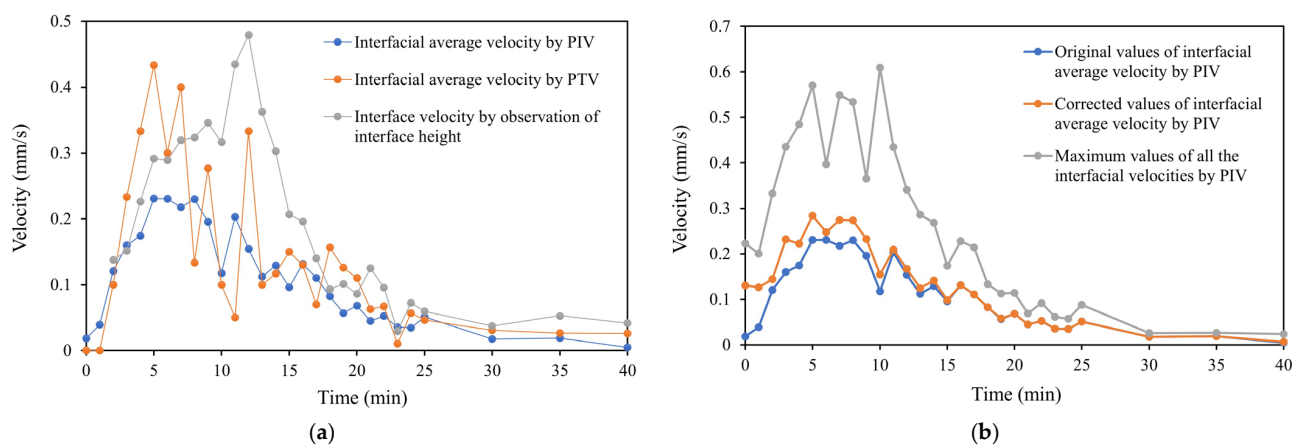


Figure 4. Time variation in interfacial average velocity calculated with PIV: (a) comparison of interfacial average velocity calculated with PIV and PTV and interface velocity based on observation of the interface height; (b) comparison of original and corrected values of the interfacial average velocity and maximum values of all the interfacial velocities, calculated with PIV.

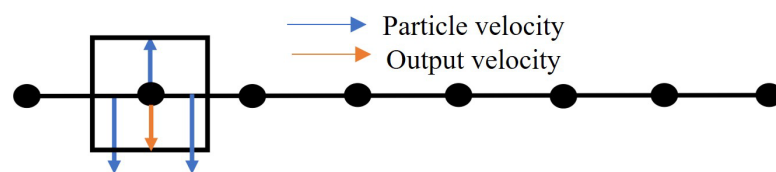


Figure 5. Schematic diagram of the mechanism of flow velocity output via PIV.

3.3. Sedimentation Turbulence Observed in PIV Analysis

Figures 6 and 7 illustrate the distribution of velocity vectors and the direction of these vectors along a horizontal line, respectively, during the sedimentation of flocculated Na-montmorillonite in a rectangular settling container with a 20 mm thickness. In Figure 7, positive degrees indicate downward flow, while negative degrees indicate upward flow. The vector maps revealed that the presence of turbulence resulted in a variety of effective velocity values, demonstrating that the flocs and the surrounding fluid move at different velocities. Additionally, they showed flow instability, with larger flocs descending and smaller flocs, along with the fluid, ascending. This is indicative of the feed-forward mechanism occurring during the sedimentation process.

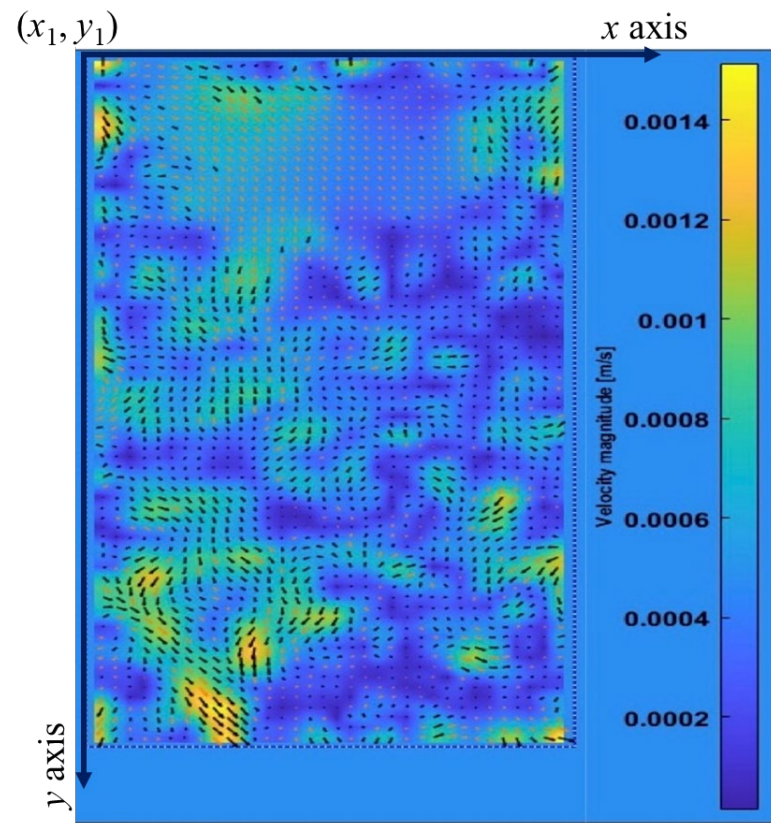


Figure 6. Distribution of velocity vectors during the sedimentation of flocculated Na-montmorillonite in a rectangular settling container with a thickness of 20 mm.

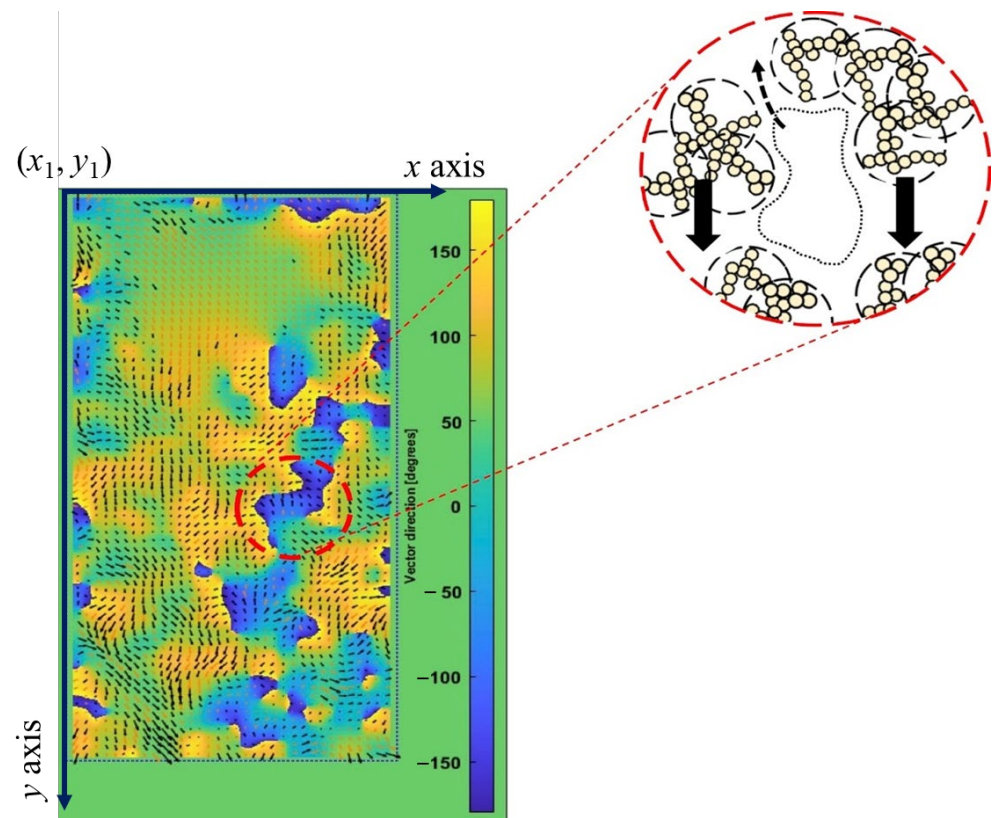


Figure 7. Distribution of vector direction along a horizontal line during the sedimentation of flocculated Na-montmorillonite in a rectangular settling container with a thickness of 20 mm.

3.4. Time Variation in Interfacial Average Velocity and RMS Velocity Fluctuation

The sedimentation turbulence was quantified for the sedimentation of flocculated Na-montmorillonite in a rectangular settling container with a 20 mm thickness. The analysis focused on the first two stages of the semi-dilute regime (i.e., flocculation and sedimentation), where flow instability begins to emerge and intensifies during the floc collapse. This instability or turbulence during the sedimentation of flocculated material results in fluctuations in velocity [24,25]. Therefore, to investigate the time variation in sedimentation turbulence, the interfacial average velocity and the root-mean-square (RMS) velocity [26] were obtained using the following equations:

$$U(y_1) = \frac{1}{N} \sum_{i=1}^N u(x_i, y_1) \quad (4)$$

$$V(y_1) = \frac{1}{N} \sum_{i=1}^N v(x_i, y_1) \quad (5)$$

$$u_{rms}(y_1) = \sqrt{\frac{1}{N} \sum_{i=1}^N (u(x_i, y_1) - U(y_1))^2} \quad (6)$$

$$v_{rms}(y_1) = \sqrt{\frac{1}{N} \sum_{i=1}^N (v(x_i, y_1) - V(y_1))^2} \quad (7)$$

x_i represents the horizontal coordinate, while y_i denotes the vertical coordinate from the interface boundary to the bottom. $U(y_1)$ and $V(y_1)$ represent the mean velocity of all points on the interface boundary for the u and v components, respectively. $u_{rms}(y_1)$ and $v_{rms}(y_1)$ represent the RMS velocity on the interface boundary for the u and v components, respectively. Figure 8 represents the time variation in the mean velocity and RMS velocity on the interface boundary for the u and v components. It was observed that the range value of the v component was greater compared with the u component, as its direction is consistent with the gravitational force and the settling Na-montmorillonite.

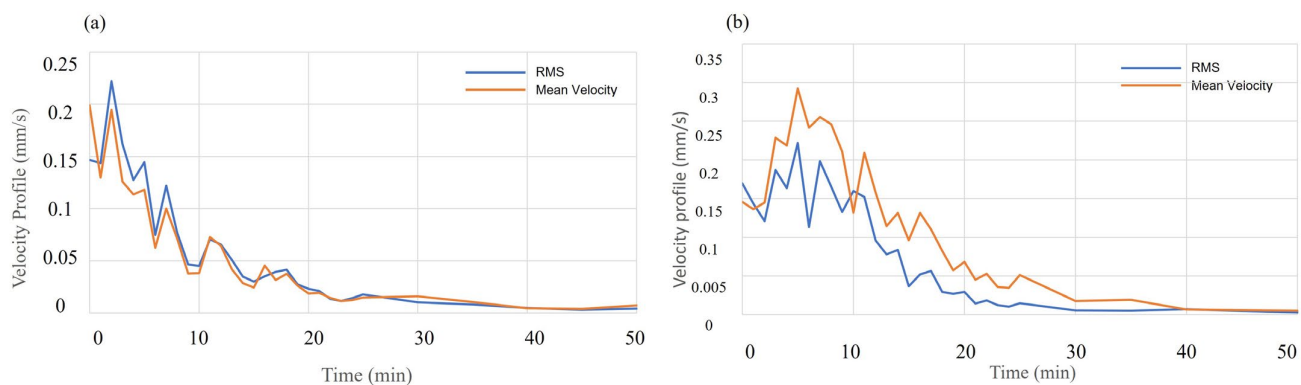


Figure 8. Time variation in the mean velocity and RMS velocity at the interface boundary during the flocculation and sedimentation stages: (a) u component; (b) v component.

At the beginning of the flocculation stage, the slighter movement of the flocculated particles results in a lower mean velocity and corresponding RMS velocity. However, during the floc collapse, the sudden downward movement of the flocculated sediment generates an upward flow, increasing the mean velocity and corresponding RMS velocity. This implies that the flow velocity fluctuation in the turbulent flow region is amplified [27]. Additionally, the larger value of u_{rms} compared with U indicates a significantly high flow instability, observed as sedimentation turbulence during the sedimentation process.

3.5. Effects of Initial Interface Height and Container Thickness on Sedimentation Behavior

In this section, we delve into the effects of initial interface heights and container thicknesses on the sedimentation behavior of flocculated Na-montmorillonite. To investigate the effects of the initial interface height, the time variation in the height of the settling interface boundary is visually represented in Figure 9. The sedimentation curve demonstrated a trend consistent with previous work, specifically referenced in [15]. This alignment was noted in the context of a 2D analysis conducted on the rectangular container. A distinct stage of initial flocculation was identified, which was more pronounced in scenarios involving higher initial suspension heights. To enhance the clarity of observations during this initial flocculation phase, the time axis in the upper right graph of Figure 9 was plotted on a logarithmic scale. The maximum settling velocity of the interface boundary is also depicted in Figure 10. The results confirmed that the maximum settling velocity increases with the initial interface height, which is caused by sedimentation turbulence. To clarify the effects of container thickness, the time variation in interfacial velocities for thicknesses of 10 mm, 15 mm, and 20 mm is represented in Figure 11. As the thickness increased, the maximum value of the interfacial average velocity also increased, and there was a tendency for the duration of the flocculation stage, i.e., the time taken to reach this maximum value, to be shortened. Previous studies have also reported that the maximum interfacial velocity is larger in cylinders with diameters ranging from 20 mm to 40 mm [17]. It is believed that the differences in maximum interfacial velocity arise from the fact that, as the thickness decreases, the wall resistance increases, reducing the downward and upward flow that promotes settling. Furthermore, for the same reason, it is hypothesized that, when the thickness becomes sufficiently large, the maximum value reaches a constant. This observation underscores the significance of the physical constraints of the experimental setup on both the sedimentation process and the characteristics of the flocs formed.

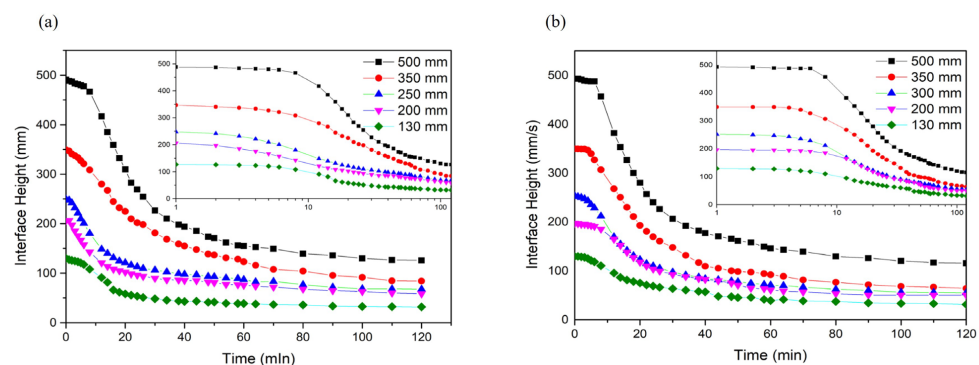


Figure 9. Time variation in the interface height as a function of initial suspension height for the sedimentation of flocculated Na-montmorillonite in rectangular settling containers with different thicknesses: (a) 20 mm; (b) 15 mm.

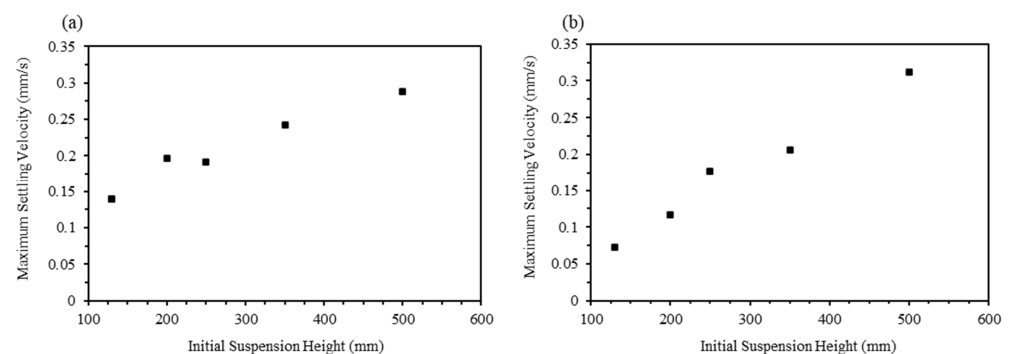


Figure 10. Maximum velocity of the moving interface height with respect to different initial suspension heights for the sedimentation of flocculated Na-montmorillonite in rectangular settling containers with different thicknesses: (a) 20 mm; (b) 15 mm.

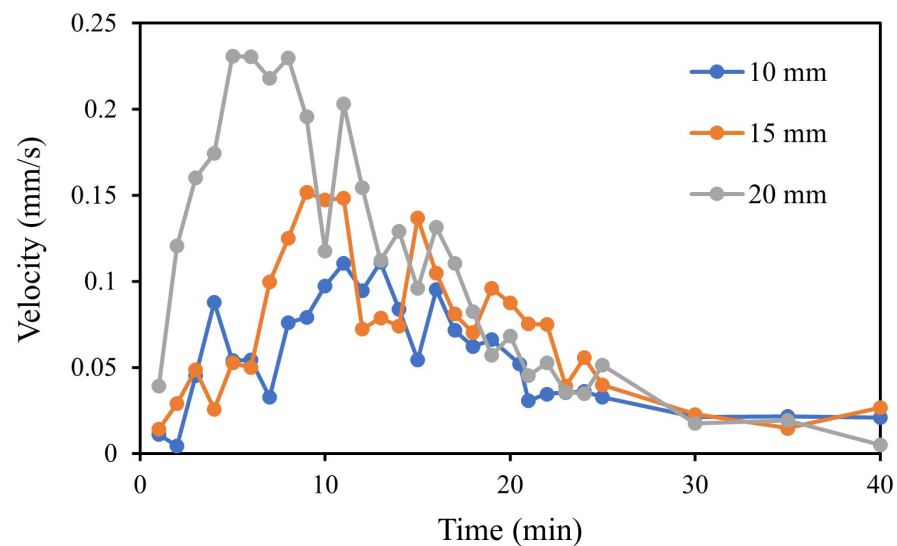


Figure 11. Time variation in the interfacial average velocities in containers with different thicknesses.

3.6. Floc Size Estimation by Fourier Analysis

Fourier analysis was applied in the vertical direction for rectangular containers with thicknesses of 10 mm, 15 mm, and 20 mm. The temporal evolution of the vertical component of the Fourier spectrum in containers with different thicknesses is presented in Figure 12. These figures illustrate the temporal changes in the spectral distribution, where the spectral distribution itself represents the frequency (amplitude) of flocs of various sizes (wave numbers). Thus, by examining Figure 12, we can visually understand the temporal changes in the size distribution of flocs during sedimentation. In cases (a), 10 mm, and (b), 15 mm, we observed temporal changes in the spectral distribution corresponding to the flocculation stage, sedimentation stage, and consolidation stage. However, in case (c), 20 mm, it was not possible to clearly observe temporal changes in the spectral distribution. This may be because the laser is emitted in a sheet-like form, and as the thickness increases, flocs not directly illuminated exist, affecting the brightness. This remains a future challenge for floc size estimation using Fourier analysis. The beginning of the sedimentation stage in case (a), 10 mm, is around 10 min, whereas in case (b), 15 mm, it is around 5 min, a trend that is consistent with Figure 11. In the flocculation stage, from approximately 0 to 10 min in case (a) and 0 to 5 min in case (b), the montmorillonite flocs appear to be uniformly distributed, resulting in a small amplitude across all wave numbers. In the settling stage, from approximately 10 to 20 min in case (a) and 5 to 20 min in case (b), there is a significant variation in amplitude. During this stage, the grown flocs undergo separation and additional flocculation because of collisions, further promoting floc growth. The sedimentation of different-sized flocs causes a large amplitude across all wave numbers. In the consolidation stage, from approximately 20 to 40 min in cases (a) and (b), compaction commences from the flocs that have settled at the bottom, and the compaction process progresses very slowly because of the weight of the flocs. As a result, the floc size gradually decreases until stabilization occurs, leading to a gradual decrease in amplitude, eventually stabilizing into a specific amplitude pattern.

Based on these observations, it can be concluded that the Fourier spectra effectively reflect the formation and collapse phenomena of the flocs.

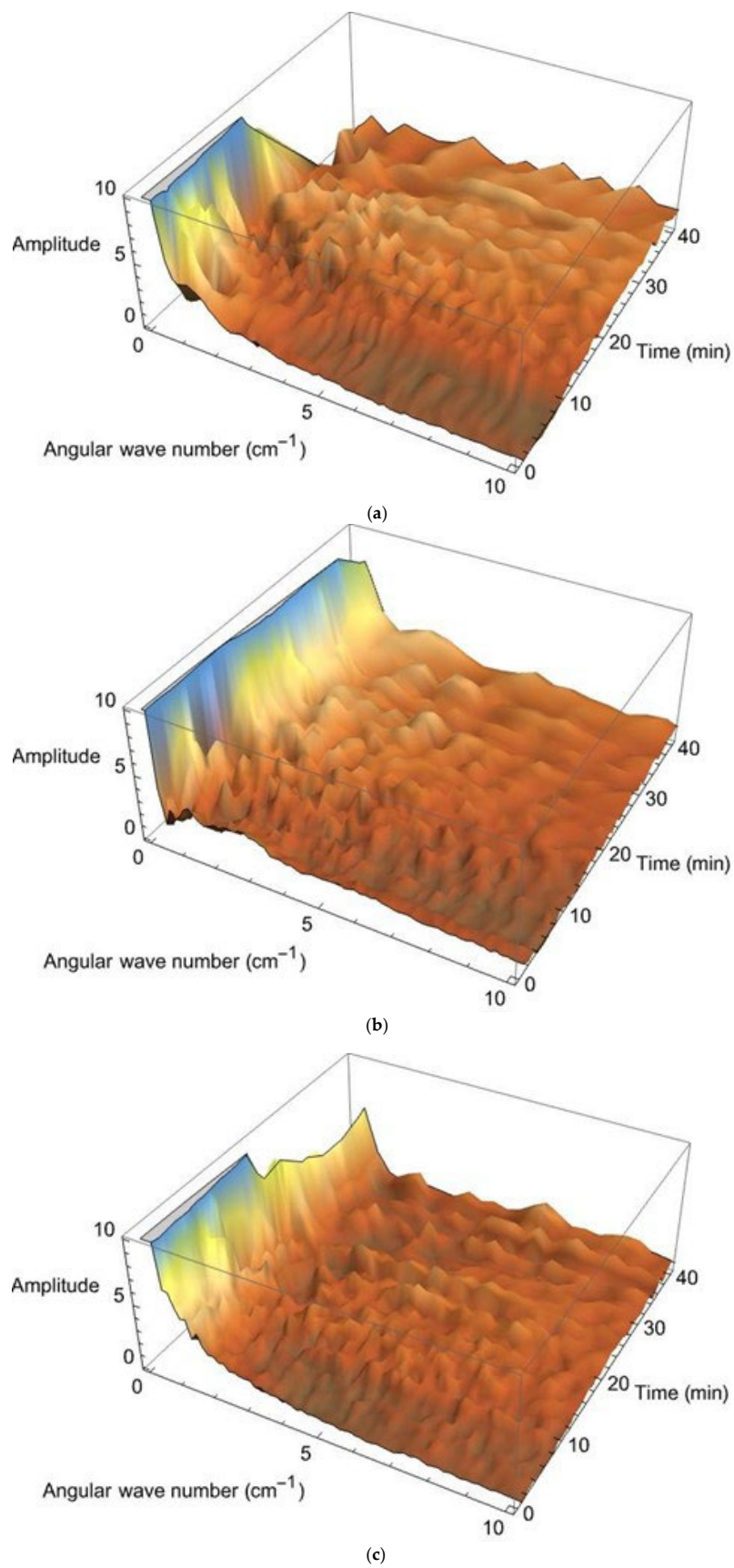


Figure 12. Temporal evolution of the vertical component of the Fourier spectrum in containers with different thicknesses: (a) 10 mm; (b) 15 mm; (c) 20 mm.

4. Conclusions

In this study, we examined the sedimentation behavior of montmorillonite flocs in a rectangular container with a narrow gap, employing a 2D system and utilizing PIV analysis. Our observations confirmed that the flow velocity obtained via PIV analysis was lower than those acquired from other methods, as illustrated in Figure 4. This discrepancy can be attributed to the fact that other methods often neglect the influence of small flocs, which possess upward flow velocities because they are entrained by sedimentation turbulence. With this consideration, the results of the PIV analysis can be deemed reliable and reflective of the actual flow velocity. Moreover, sedimentation turbulence was observed during the settling of the flocculated Na-montmorillonite flocs in the 2D flow. We noted a monotonous increase in maximum settling velocity as a function of the initial suspension height, as depicted in Figure 10. Additionally, an increase in the thickness of the rectangular containers correlated with an increase in the maximum settling velocity and a decrease in the duration from the flocculation stage to the settling stage, as depicted in Figure 11. Prior experiments using cylinders have also indicated a similar trend, which can be attributed to the fact that a small container size limits sedimentation behavior by reducing both downward and upward flow because of large wall resistance. This mechanism suggests that, when the thickness becomes sufficiently large, the maximum value may reach a constant. However, this needs to be verified in further studies. The time variation in the interfacial average velocity—alongside the corresponding RMS turbulence fluctuation of particle movement within the flow of the interface—was analyzed, revealing the sedimentation turbulence observed during the sedimentation process, as showcased in Figure 8. Additionally, the temporal evolution of the vertical component of the Fourier spectrum illustrated the formation and collapse phenomena of the flocs, as demonstrated in Figure 12. In the flocculation stage, the montmorillonite flocs were uniformly distributed, resulting in a small amplitude across all wave numbers. During the settling stage, significant amplitude variations were observed, with a large amplitude across all wave numbers, because of the sedimentation of differently sized flocs resulting from the collisions, separation, and flocculation of the flocs. In the consolidation stage, there was a gradual decrease in amplitude, which corresponded to a reduction in floc size. This trend can be attributed to the slow process of compaction.

Author Contributions: Conceptualization, H.K., Y.A. (Yasuhisa Adachi) and Y.A. (Yohei Asada); methodology, K.Y. and H.K.; software, K.Y. and H.K.; validation, K.Y., M.E.B.G., J.L. and H.K.; formal analysis, K.Y. and H.K.; investigation, M.R., K.Y. and H.K.; resources, K.Y. and H.K.; data curation, K.Y. and H.K.; writing—original draft preparation, M.R., K.Y. and H.K.; writing—review and editing, Y.A. (Yasuhisa Adachi) and Y.A. (Yohei Asada); visualization, M.R., K.Y., H.K., Y.A. (Yasuhisa Adachi) and Y.A. (Yohei Asada); supervision, H.K., Y.A. (Yasuhisa Adachi) and Y.A. (Yohei Asada); project administration, H.K. and Y.A. (Yasuhisa Adachi); funding acquisition, H.K. and Y.A. (Yasuhisa Adachi). All authors have read and agreed to the published version of the manuscript.

Funding: This research was partially funded by JSPS KAKENHI Grant Number 22H00387, “Engineering Novel Approaches to Soil and Water Environments Based on Analysis of Colloid Aggregation” (Principal Investigator: Yasuhisa Adachi). We express our gratitude for this support.

Data Availability Statement: Data are contained within the article.

Conflicts of Interest: The authors declare no conflicts of interest.

References

1. Guibai, L.I.; Gregory, J. Flocculation and sedimentation of high-turbidity waters. *J. Water Res* **1991**, *25*, 1137–1143. [[CrossRef](#)]
2. Chassagne, C. *Introduction to Colloid Science: Applications to Sediment Characterization*; TU Delft OPEN: Delft, The Netherlands, 2019. [[CrossRef](#)]
3. Uchiyama, T.; Yamamoto, K.; Yokoyama, K. Study on the Phenomenon of the Settling Rate Increasing of the Suspended Sediment around the Salinity Front in the Chikugo River Estuary, Japan. *J. Jpn. Soc. Civ. Eng. Ser. B2 (Coast. Eng.)* **2010**, *66*, 1001–1005. [[CrossRef](#)]
4. Droppo, I.G.; Leppard, G.G.; Liss, S.N.; Milligan, T.G. *Flocculation in Natural and Engineered Environmental Systems*; CRC Press: Boca Raton, FL, USA, 2004.

5. Adachi, Y. Aspects of colloid and interface in the engineering science of soil and water with emphasis on the flocculation behavior of model particles. *Paddy Water Environ.* **2019**, *17*, 203–210. [\[CrossRef\]](#)
6. Wakai, T.; Kaneki, R.; Itakura, Y.; Banno, M. Water Quality and Loads of Rivers during Puddling Transplanting Period. *J. Jpn. Soc. Hydrol. Water Resour.* **2005**, *18*, 167–176. [\[CrossRef\]](#)
7. Sudo, M.; Miki, T.; Masuda, Y. Research on characteristics of turbid water effluent from paddy fields during the paddling and the transplanting period. *Trans. Jpn. Soc. Irrig.* **2010**, *77*, 113–119.
8. Winterwerp, J.C.; Walther, G.M.V.K. *Introduction to the Physics of Cohesive Sediment in the Marine Environment*, 1st ed.; Elsevier: Amsterdam, The Netherlands, 2004; ISBN 0-444-51553-4.
9. Imai, G. Experimental studies on sedimentation mechanism and sediment formation of clay materials. *Soils Found.* **1981**, *21*, 7–20. [\[CrossRef\]](#)
10. Kynch, G.J. A theory of sedimentation. *Trans. Faraday Soc.* **1952**, *48*, 166–176. [\[CrossRef\]](#)
11. Davis, R.H.; Acrivos, A. Sedimentation of noncolloidal particles at low Reynolds numbers. *Annu. Rev. Fluid Mech.* **1985**, *17*, 91–118. [\[CrossRef\]](#)
12. Concha, F.; Bustos, M.C. Settling velocities of particulate systems, 6. Kynch sedimentation processes: Batch settling. *Int. J. Miner. Process.* **1991**, *32*, 193–212. [\[CrossRef\]](#)
13. Richardson, J.F.; Zaki, W.N. The sedimentation of a suspension of uniform spheres under conditions of viscous flow. *Chem. Eng. Sci.* **1954**, *3*, 65–73. [\[CrossRef\]](#)
14. Michaels, A.S.; Bolger, J.C. Settling rates and sediment volumes of flocculated kaolin suspensions. *Ind. Eng. Chem. Fundam.* **1962**, *1*, 24–33. [\[CrossRef\]](#)
15. Ghazali, M.E.B.; Argo, Y.; Kyotoh, H.; Adachi, Y. Effect of the concentration of NaCl and cylinder height on the sedimentation of flocculated suspension of Na-montmorillonite in the semi-dilute regime. *Paddy Water Environ.* **2020**, *18*, 309–316. [\[CrossRef\]](#)
16. Li, J.; Adachi, Y. Analysis of sedimentation behavior of flocculated Na-Montmorillonite in a Semi-dilute Regime—Effects of the container height. *J. Jpn. Soc. Soil Phys.* **2023**, *accepted*.
17. Ghazali, M.E.B.; Adachi, Y. Container size effects on the validity for the concept of sedimentation turbulence studied using coagulated suspension of Na-montmorillonite in the semi-dilute regime. *Colloids Surf. A Physicochem. Eng. Asp.* **2021**, *630*, 127567. [\[CrossRef\]](#)
18. Van Olphen, H.; Hsu, P.H. An introduction to clay colloid chemistry. *Soil Sci.* **1978**, *126*, 59. [\[CrossRef\]](#)
19. Abend, S.; Lagaly, G. Sol–gel transitions of sodium montmorillonite dispersions. *Appl. Clay Sci.* **2000**, *16*, 201–227. [\[CrossRef\]](#)
20. Nezu, I.; Sanjou, M. PIV and PTV measurements in hydro-sciences with focus on turbulent open-channel flows. *J. Hydro-Environ. Res.* **2011**, *5*, 215–230. [\[CrossRef\]](#)
21. Sueto, J.; Nakaishi, K. Thixotropic behaviors of Sodium and Calcium Montmorillonite at salt concentration in the vicinity of 0.3 M. *Clay Sci.* **1992**, *8*, 349–353.
22. Liu, Z.; Jiao, J.; Zheng, Y. Study of axial velocity in gas cyclones by 2D-PIV, 3D-PIV, and simulation. *China Particuology* **2006**, *4*, 204–210. [\[CrossRef\]](#)
23. Stamhuis, E.; Thielicke, W. PIVlab—towards user-friendly, affordable and accurate digital particle image velocimetry in MATLAB. *J. Open Res. Softw.* **2014**, *2*, e30. [\[CrossRef\]](#)
24. Boyer, C.; Roy, A.G.; Best, J.L. Dynamics of a river channel confluence with discordant beds: Flow turbulence, bed load sediment transport, and bed morphology. *J. Geophys. Res. Earth Surf.* **2006**, *111*. [\[CrossRef\]](#)
25. Zanke, U.C.E. On the influence of turbulence on the initiation of sediment motion. *Int. J. Sediment Res.* **2003**, *18*, 17–31.
26. Kneller, B.C.; Bennett, S.J.; McCaffrey, W.D. Velocity and turbulence structure of density currents and internal solitary waves: Potential sediment transport and the formation of wave ripples in deep water. *Sediment. Geol.* **1997**, *112*, 235–250. [\[CrossRef\]](#)
27. Buckles, J.; Hanratty, T.J.; Adrian, R.J. Turbulent flow over large-amplitude wavy surfaces. *J. Fluid Mech.* **1984**, *140*, 27–44. [\[CrossRef\]](#)

Disclaimer/Publisher’s Note: The statements, opinions and data contained in all publications are solely those of the individual author(s) and contributor(s) and not of MDPI and/or the editor(s). MDPI and/or the editor(s) disclaim responsibility for any injury to people or property resulting from any ideas, methods, instructions or products referred to in the content.